Heliyon 10 (2024) e33801

Contents lists available at ScienceDirect

Heliyon

journal homepage: www.cell.com/heliyon

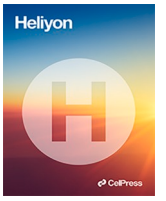

Research article

# Influence of natural polysaccharides on the morphology and properties of hybrid vaterite microcrystals

Nadezhda G. Balabushevich [a], Liliya N. Maltseva [a,b], Lyubov Y. Filatova [a], Daniil V. Mosievich [a,b], Pavel I. Mishin [a], Margarita E. Bogomiakova [b], Olga S. Lebedeva [b], Marina A. Murina [b], Dmitry V. Klinov [b,c], Ekaterina A. Obraztsova [b], Zaira F. Kharaeva [d], Roxalana K. Firova [b], Daria V. Grigorieva [e], Irina V. Gorudko [e], Oleg M. Panasenko [b,f], Elena V. Mikhalchik [b,*]

[a] *Lomonosov Moscow State University, Department of Chemistry, Leninskiye Gory 1–3, 119991, Moscow, Russia*
[b] *Lopukhin Federal Research and Clinical Center of Physical-Chemical Medicine of Federal Medical Biological Agency, Malaya Pirogovskaya st. 1a, 119435, Moscow, Russia*
[c] *The Peoples' Friendship University of Russia (RUDN University), Miklukho-Maklaya str. 6, 117198, Moscow, Russia*
[d] *Kabardino-Balkarian State University named after H.M. Berbekov, Faculty of Medicine, Inessa Armand st. 1a, 360004, Nalchik, Kabardino-Balkarian Republic, Russia*
[e] *Belarusian State University, Nezavisimosti av. 4, 220030, Minsk, Belarus*
[f] *Pirogov Russian National Research Medical University, Ostrovityanova st. 1, 117997, Moscow, Russia*

ARTICLE INFO

*Keywords:*
Calcium carbonate (vaterite)
Biocompatibility
Antioxidant properties
Protein adsorption
Enzyme activity
Drug delivery

ABSTRACT

Co-precipitation of biopolymers into calcium carbonate crystals changes their physicochemical and biological properties. This work studies hybrid microcrystals of vaterite obtained in the presence of natural polysaccharides, as carriers for the delivery of proteins and enzymes. Hybrid microcrystals with dextran sulfate, chondroitin sulfate, heparin, fucoidan, and pectin were obtained and compared. The impact of polysaccharides on the morphology (particle diameter, surface area, nanocrystallite and pore size), polysaccharide content and surface charge of hybrid microcrystals was studied. Only microcrystals with fucoidan and heparin exhibited antioxidant activity against $^{\bullet}$OH radical. The surface charge and pore size of the hybrid microcrystals affected the sorption of albumin, catalase, chymotrypsin, mucin. A decrease in the catalytic constant and Michaelis constant was observed for catalase sorbed on the hybrid crystals. The biocompatibility of microcrystals depended on the nature of the included polysaccharide: crystals with sulfated polysaccharides increased blood plasma coagulation but not platelet aggregation, and crystals with dextran sulfate had the greatest cytotoxicity against HT-29 cells but not erythrocytes. Hybrid microcrystals with all polysaccharides except chondroitin sulfate reduced erythrocyte lysis in

*Abbreviations:* ADP, adenosine diphosphate; PRP, platelet-rich plasma; LCL, luminol chemiluminescence; IBC, iron-binding capacity; APTT, activated partial thromboplastin time; polysaccharides, DS; dextran sulfate, CS; chondroitin sulfate, HE; heparin, FU; fucoidan, PE; pectin, CC; microcrystals of vaterite (calcium carbonate), hybrid microcrystals with polysaccharides; CCDS, with dextran sulfate; CCCS, with chondroitin sulfate; CCHE, with heparin; CCFU, with fucoidan; and CCPE, with pectin; SEM, scanning electron microscopy; BET, Brunauer–Emmett–Teller method; $D_{crystal}$, diameter of microcrystals; $D_{nanocrystalline}$, diameter of nanocrystallines; $D_{pores}$, diameter of pore; $k_{cat}$, catalytic constant; $K_m$, Michaelis constant; $q_e$, equilibrium adsorption capacity of the microcrystals; $S$, microcrystal area; $v_{max}$, is the maximum reaction rate; $V_{pores}$, pore volume.

* Corresponding author.
*E-mail addresses:* lemik2007@yandex.ru, mihalchik@rcpcm.ru (E.V. Mikhalchik).

https://doi.org/10.1016/j.heliyon.2024.e33801
Received 28 February 2024; Received in revised form 2 May 2024; Accepted 27 June 2024
Available online 28 June 2024

vitro compared with vaterite crystals. The obtained results enable to create novel carriers based on hybrid vaterite crystals with polysaccharides, beneficial for the delivery of protein drugs.

## 1. Introduction

Nowadays, special attention is paid to the development of alternative means of drug delivery with low cost and the necessary biological activity. Mineral particles made of clay, halloysite, apatite, and calcium carbonate find use in various biomedical applications due to the presence of special physicochemical properties, low toxicity, biocompatibility, or biodegradability [1–5]. The production costs of calcium carbonate are very low [2], and its vaterite modification differs from other polymorphic forms calcite and aragonite by its special properties. The spherical shape and adjustable sizes in the range from submicron up to tens of micron [6], pH sensitivity (better release of substances at lower pH) of vaterite crystals may be important for controlled drug and gene delivery as well as targeted cancer therapy, since cancer cells have a lower pH environment compared to healthy cells [7,8]. The high affinity of vaterite crystals for mucin [9] makes them promising carriers for drug delivery through mucous membranes [10,11], including intranasal [12], pulmonary [13], oral [14] or ophthalmic [15] administration. Unlike other popular drug delivery vehicles in the form of metal nanoparticles, synthetic copolymers, and cationic lipids, calcium carbonate has no potential material safety issues and is marketed as an FDA-approved antacid (Section 331.11b), digestive, antidiarrheal, or weight control drug (Section 310.545) [1].

Vaterite crystals have a porous morphology and a well-developed internal structure but are the least stable polymorph of calcium

**Table 1**
Characteristics of polysaccharides used in the work.

| Polysaccharide | Structure | Biological activity |
|---|---|---|
| Dextran sulfate (DS) | 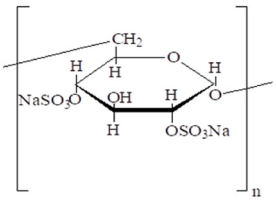 | anticoagulant [30,31] |
| Chondroitin sulfate (CS) | 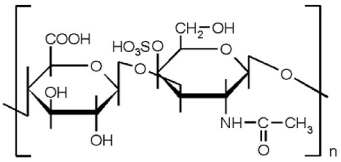 | anti-inflammatory [32], antioxidant [33,34], immunomodulating [35] |
| Heparin (HE) | 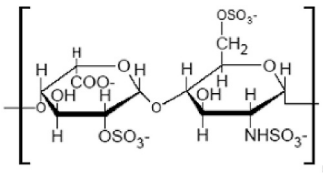 | antiviral [36], antioxidant [37], anti-inflammatory [38], anticancer [39] |
| Fucoidan (FU) | 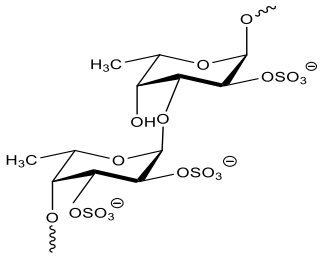 | antioxidant [40,41], anticoagulant [42], antiviral [43], anticancer [44] |
| Pectin (PE) | 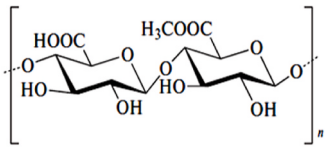 | antioxidant [45], immunomodulating [46], anti-inflammatory [47] |

carbonate. Vaterite has ideal mechanical, physical and chemical properties for incorporating substances of various nature, including low and high molecular weight drugs, which can be loaded using coprecipitation during crystal fabrication or adsorption into prepared crystals [16,17]. Among the disadvantages of vaterite are small inclusion and rapid release of positively charged molecules, low stability in solutions, and rapid recrystallization into more thermodynamically stable calcite. These disadvantages can be eliminated by additional introduction of polymers during the formation of crystals to obtain so-called "hybrid" crystals of vaterite. Modification of the vaterite matrix with biopolymers (cellulose [18], chitosan and its derivatives [19–21], alginate [22], low molecular weight heparin [23,24], dextran sulfate [25,26], pectin [27], mucin [28] changed the surface charge of the particles, increased the surface area and porosity, and, as a result, not only increased incorporation and retention of cationic drugs (including proteins and enzymes), but also produced additional therapeutic effects. In the body, carrier particles are inevitably exposed to the components of biological media and may elicit a response from the immune system. In this regard, it is important to know to what extent the modification of vaterite microcrystals by biopolymers affects the incorporation of therapeutically important proteins and enzymes. It is also necessary to study the interaction of polysaccharide-modified vaterite with components of biological media and body cells.

Natural polysaccharides due to the availability and renewability of raw materials, biodegradability and biocompatibility attract special attention for the creation of protein delivery vehicles [29]. It should be noted that most polysaccharides are polydisperse, and their molecular weight and degree of sulfation depend on the source of raw materials and polymer extraction conditions. Polysaccharides are hydrophilic, non-toxic and can be degraded by enzymes of human body and gastrointestinal bacteria. In our work, well known sulfated polysaccharides (dextran sulfate, chondroitin sulfate, heparin, and fucoidan) and non-sulfated polysaccharide pectin (Table 1), negatively charged under physiologic conditions due to sulfo and carboxyl groups in their structure, which have a wide range of biological properties (antioxidant, anticoagulative, anti-inflammatory, immunomodulating, antiviral, anticancer, etc.) were selected for inclusion in vaterite microcrystals [30–45].

Dextran sulfate (DS) is produced by sulfation of dextran synthesized by bacteria [48]. Chondroitin sulfate (CS) from mammals and invertebrates is a typical glycosaminoglycan and the proteoglycan component of the extracellular matrix [49]. Clinical study revealed the safety of chondroitin sulfate administration and almost no side effects. Heparin (HE) is a highly sulfated polydispersed glycosaminoglycan whose polysaccharide chain consists of repeating dimers of L-iduronic acid (IdoA) or glucuronic acid (GlcA) and N-acetylglucosamine (GlcNAc) [50]. Heparin is the most widely used anticoagulant drug in the world, and it is derived from bovine lungs or pig intestinal mucosa. The main component of fucoidan (FU) from brown algae and echinoderms is sulfated α-L-fucose residues, but it can also include other monosaccharides, such as galactose, mannose, xylose, and uronic acids [51]. This biopolymer has a branched structure with an irregular alternation of sulfated/acetylated monosaccharides with α(1 → 3) glycosidic linkages or alternating α(1 → 3), α(1 → 4) in the main chain. Pectin (PE) is a non-sulfated polysaccharide whose main chain consists of alternating links of D-galacturonic acid and α-1,2-L-rhamnose connected by α(1 → 4) glycosidic bond, as well as various uncharged monosaccharides: arabinose, galactose, etc. [52]. Pectin is part of the cell wall of higher plants, reaching up to one third of all dry substances contained in the cell wall.

So far, the comprehensive comparison of the effect of the nature of polysaccharides on the physicochemical and antioxidant properties, biocompatibility, and cytotoxicity of hybrid microcrystals of vaterite, and on their interaction with biologically active substances is important for further progress in the development of drug delivery systems [53,54].

The adsorption of human serum albumin and high molecular weight glycoprotein mucin, which is the main component of all mucosal surfaces, was studied when analyzing the interaction of hybrid microcrystals of vaterite as drug carriers in delivery vehicles with components of biological media.

Since vaterite modified with natural polysaccharides can be of interest as carrier for the delivery of therapeutically important proteins and enzymes, the adsorption of anionic antioxidant enzyme catalase (500 kDa, pI 5.4) and cationic pancreatic proteolytic enzyme chymotrypsin (25 kDa, pI 8.8) onto hybrid microparticles was compared. In order to evaluate efficacy of inclusion of the enzymes, also their activity was assessed. Kinetic parameters of the immobilized enzyme in the hydrogen peroxide decomposition reaction were determined for the adsorbed catalase.

So, our work aims to compare the properties of hybrid vaterite microcrystals with polysaccharides and to predict their possible use as carriers in drug delivery vehicles. The hybrid microcrystals were prepared and characterized by: (1) their physical-chemical properties (particle diameter, surface area, nanocrystallite and pore size, polysaccharide content, surface charge, antioxidant activity); (2) biocompatibility with respect to blood plasma coagulation, platelet aggregation, blood erythrocytes and HT-29 cells related to intestinal epithelium; (3) their protein-adsorbing capacity towards mucin and albumin which are the major proteinaceous components of mucosa and blood plasma; (4) adsorbing capacity towards therapeutically important enzymes catalase and chymotrypsin as perspective candidates for delivery with hybrid microcrystals. Among the studied polysaccharides there were dextran sulfate, chondroitin sulfate, heparin, fucoidan, and pectin.

X-ray phase analysis, thermogravimetric analysis and electrophoretic laser light scattering and nitrogen sorption–desorption, and iron binding capacity and hydroxyl-scavenging activity in Fenton reaction were used for physicochemical characterization of the hybrid crystals. To analyze the biocompatibility of vaterite microcrystals we studied their effect on blood plasma coagulation and platelet aggregation in platelet-rich plasma (PRP). In addition, we evaluated cytotoxicity in a hemolysis model [55] and, given the possibility of oral administration, against the HT-29 cell line. The colorectal cancer cell line HT-29 is related to the intestinal epithelium [56] and has been used in colitis models in vitro [57].

## 2. Materials and methods

### 2.1. Materials

Anhydrous calcium chloride, ≥93.0 % (C1016), anhydrous sodium carbonate, ≥99.0 % (S7795), CS type A sodium salt from bovine trachea, 10–30 kDa (C8529), FU from *Fucus vesiculosus*, 30–100 kDa (F-5631), PE from apple, 6.7 % for Methoxy groups,74.0 % for Galacturonic Acid (P-8471), mucin from porcine stomach, ≈600 kDa, Type III (M), bovine liver catalase, albumin from human serum (Fraction V), hydrogen peroxide solution, N-benzoyl-L-tyrosine-*p*-nitroanilide, luminol, lucigenin (Sigma–Aldrich, USA, China); DS *Leuconostoc* ssp. $M_r$ ≈500 kDa, containing 2.3 sulfo groups per unit (31395), chymotrypsin from bovine pancreas (Fluka, Germany); HE, 10–20 kDa (Spofa, Czech Republic). The Olvex-LDH kit, Iron-4-Olvex kit were purchased from LLC (Olveks Diagnosticum, SPb, Russia).

All chemicals used for the preparation of buffer solutions were at least laboratory grade and purchased from Sigma–Aldrich. All other chemicals were used without further purification. Double distilled water was used in all experiments.

### 2.2. Fabrication of CC and hybrid microcrystals

Microcrystals of vaterite (CC) and hybrid microcrystals with all polysaccharides were obtained according to the method [28] with some modifications. For the fabrication of hybrid microcrystals, 3 mL of 1 M $CaCl_2$, 7.5 mL 10 mg $mL^{-1}$ of polysaccharide in 0.1 M Tris buffer, 1.5 mL water was stirred for 10 min followed by the addition of 3 mL of 1 M $Na_2CO_3$. Stirring was continued for 45 s, then the suspension was left for 15 min without stirring for precipitation. CC microcrystals were fabricated following the same procedure without addition of polysaccharide into the $CaCl_2$ solution. After precipitation of the crystals, the supernatant solutions were separated by centrifugation for 1 min at 1000 rpm; the precipitates were washed three times with double distilled water and lyophilized.

### 2.3. Characterization of the microcrystals

For scanning electron microscopy (SEM) microcrystals were deposited onto silicon wafers and characterized using a Zeiss Merlin microscope (Zeiss, München, Germany). SEM accelerating voltage was 1–2 kV. The statistical image processing was performed through ImageJ when counting 100 microcrystals for each preparation and microcrystals diameter ($D_{crystal}$) was assayed. Diameter of nanocrystallines ($D_{nanocrystalline}$) was calculated using Gwiddion software.

The sulfur content in microcrystals was analyzed by energy disperse X-ray spectroscopy during SEM measurements using an additional module Oxford Instruments INCAx-act. Elevated accelerating voltage of 10–15 kV was used to record the data.

An X-ray diffraction analysis of the microparticles was performed using a Miniflex 600 (Rigaku, Japan) with a silicon drift detector on powdered samples using Cu Ka 1.5418 Å radiation and a Ni filter with 2θ from 20° to 60°. The molar percentages of vaterite and calcite polymorphs were determined using the equations derived from the research conducted by Ref. [58]: using Eq. (1):

$$I_c^{104} / I_v^{110} = 7.691 * X_c / X_v \quad (1)$$

where 7.691 is the proportionality constant of the calcite and vaterite polymorph mixture, IC 104 represents the intensity of the calcite diffraction plane (104), while IV 110 represents the intensity of the vaterite diffraction plane (110). XC represents the molar fraction of calcite, and XV represents the molar fraction of vaterite (XC + XV = 1).

Thermogravimetric analysis (TGA) was carried out using a TGA/DSC analyzer (SDT Q600, Thermo Fisher Scientific, TA Instruments). The samples (30 mg) were heated from 30 to 1000 °C at a heating rate of 10 °C $min^{-1}$ under an air flow with the rate of 100 mL $min^{-1}$.

The porosity of microcrystals was studied by low-temperature nitrogen adsorption–desorption on ASAP-2000 setup (Micromeritics, Norcross, GA, USA). The specific surface area was estimated by Brunauer–Emmett–Teller (BET) method, the pore size was calculated using Barrett–Joyner–Halenda method. The porosity of the vaterite microparticles was studied by low-temperature $N_2$ adsorption–desorption by the BET method on ASAP-2000 setup (Micromeritics, USA). The samples were preliminarily subjected to vacuum treatment at room temperature to a residual pressure of $2 \times 10^{-6}$ bar. The isotherms were recorded at 196 °C as the dependences of the volume of the sorbed $N_2$ ($cm^3$ $g^{-1}$) on the relative pressure $p/p_0$, where $p_0$ is the pressure of saturated $N_2$ vapor at 196 °C. The characteristics of the samples – crystal area ($S$), pore volume ($V_{pores}$), and pore size ($D_{pores}$) – were calculated using a standard software package.

The ζ-potential of biopolymers and microcrystals and hydrodynamic diameter of mucin and proteins was measured using Zetasizer (Nano ZS, Malvern, UK) and estimated using Smoluchowski equation and Stokes–Einstein equation, respectively.

### 2.4. Sorption of proteins and mucin on microcrystals

The suspension containing 40 mg $mL^{-1}$ microcrystals and 1.0 mg $mL^{-1}$ of proteins or mucin in 0.05 M Tris buffer (pH 7.0) was incubated under the stirring at 300 rpm for 30 min and centrifuged for 2 min at 2000 rpm. The precipitates were washed twice with 0.05 M Tris buffer. Control suspensions of the microcrystals did not contain protein. The content of the catalase immobilized on the microcrystals was calculated based on the concentration of the catalase in the supernatant and washing solutions, which were determined in comparison with the control suspensions at a wavelength of 280 nm for protein or 260 nm for mucin. The equilibrium

adsorption capacity of the microcrystals ($q_e$, mg $g^{-1}$) was calculated using Eq. (2):

$$q_e = (c_o - c_e)*V/m, \quad (2)$$

where $c_o$ and $c_e$ are the initial and equilibrium concentrations of catalase, respectively (mg $mL^{-1}$), $V$ is the volume of the suspension (mL), and $m$ is the mass of the microparticles (g).

### 2.5. Catalase activity

Catalase activity was assayed as described earlier [59]. Catalase solution or suspension of the microcrystals loaded with catalase was diluted with 0.05 M Tris buffer (pH 7.0 to the same protein concentration 0.005–0.010 mg $mL^{-1}$ [59]. An aliquot of 820–870 μL of 0.05 M Tris buffer (pH 7.0) was mixed with 30–80 μL of diluted catalase solution and 100 μL of 176 mM $H_2O_2$ solutions reaching the total volume of the reaction mixture of 1000 μL. For the measurement of the activity of immobilized catalase, a control experiment was always set up with the same concentration of CC or hybrid microcrystals, which did not contain catalase. Optical density at a wavelength of 240 nm was recorded for 60 s.

$K_m$ and $v_{max}$ for catalase were determined using Linuiver–Burke coordinates, the catalytic constant ($k_{cat,}$ $s^{-1}$) was calculated using Eq. (3):

$$k_{cat} = v_{max} / c_{Cat}, \quad (3)$$

where $v_{max}$ is the maximum reaction rate (M $s^{-1}$); $c_{Cat}$ is the concentration of catalase active centers, M; 60 is the measurement time (s).

The concentration of catalase active centers was determined after measuring the absorbance in solutions at 280 and 410 nm using Eq. (4):

$$c_{Cat} = A_{410} * c_0 / A_{280}, \quad (4)$$

where $A_{410}$ is absorbance at 410 nm; $A_{280}$, absorbance at 280 nm, and $c_0$ is concentration of protein in solution (M).

### 2.6. Chymotrypsin activity

Chymotrypsin activity was assayed as described earlier [60]. Chymotrypsin or suspension of microcrystals loaded with chymotrypsin were diluted to the same protein concentration. 0.1–0.2 mg $mL^{-1}$. Then 950 mL of 0.05 M Tris buffer (pH 7.8) and 20 μL of chymotrypsin solution (pH 3.0 or 7.4) diluted to a concentration of 0.1–0.2 mg $mL^{-1}$ or a suspension of microcrystals in 0.05 M Tris buffer (pH 7.8) were mixed with 30 μL of a 0.8 mg $mL^{-1}$ solution of N-benzoyl-*L*-tyrosine-*p*-nitroanilide in acetonitrile. In control samples, instead of chymotrypsin solutions, 0.05 M Tris buffer or suspensions of pristine CC microcrystals, diluted similarly to the microcrystals with the enzyme, were added. The obtained samples were incubated for 20 min at 25°C and stirring at 550 rpm. The suspensions were centrifuged for 1 min at 3000 rpm, the supernatant solution was separated, and the optical density was measured at a wavelength of 410 nm. The relative activity of chymotrypsin in solutions and in suspensions of microcrystals, equalized by protein content, was calculated as the ratio of the optical density in the samples (minus the optical density in control experiments) to the optical density of the samples of the chymotrypsin solution with pH 3.0.

### 2.7. Anticoagulant activity

For the analysis of anticoagulant properties of the microcrystals, rabbit blood was used (approved by the ethical committee of Lopukhin Federal Research and Clinical Center of Physical-Chemical Medicine (Protocol No. 2022/10/05-1). Experiments were performed on platelets contained in PRP, withdrawn from the rabbit's marginal ear vein. The blood was stabilized with 3.8 % sodium citrate solution at a ratio 9 : 1 by volume and centrifuged for 15 min at 460 *g*, and the supernatant was collected. To 270 μL of supernatant, 30 μL of microcrystal suspension in 0.15 M NaCl was added and incubated for 3 min. Platelet aggregation was induced by administration of 3 μM adenosine diphosphate and recorded by the Born turbidimetric method on a Biola analyzer (Biola, Russia). The quantitative indicator of platelet aggregation ability was the maximum change in light transmission of their suspension 5–7 min after agonist administration. Platelet aggregation was expressed as % of control samples.

To determine the value of activated partial thromboplastin time (APTT), 20 μL of microcrystal suspension was added to 80 μL of rabbit blood plasma, the mixture was incubated for 1 min at 37 °C, 100 μL of a mixture of soybean phospholipids and ellagic acid was added, incubated for 2 min at 37 °C, 100 μL of 0.025 M $CaCl_2$ was added, and the time of clot formation was recorded. Measurement of plasma clotting time under particle action was performed on a Minilab-701 coagulometer (Unimed, Russia) and referred to the control value.

### 2.8. Haemolysis

Blood samples were withdrawn from healthy volunteers ($n = 10$), with their informed consent, in accordance with the protocol approved by the ethical committee of Lopukhin Federal Research and Clinical Center of Physical-Chemical Medicine (protocol No. 2022/10/05). Erythrocytes were obtained by centrifugation of the blood for 10 min at 1000 rpm and washed with 0.15 M NaCl. A 160 μL-aliquot of 0.15 M NaCl was mixed with 40 μL of washed erythrocytes and 40 μL of a suspension of microcrystals, 20 mg $mL^{-1}$. A

sample containing 200 μL of $H_2O$ and 40 μL of red blood cells was used as a positive control. The samples were incubated for 2 h at 37° C and centrifuged for 10 min at 1000 rpm, then 150 μL of supernatant was taken and the absorbance was measured at 540 nm using Ascent plate spectrophotometer (Thermo Electron Corporation, USA). The results were presented as % of positive control.

### 2.9. Cytotoxicity towards HT-29 cells

Cells HT-29 (cell line HTB-38™, obtained from the ATCC cell repository) were cultured according to the standard technique in culture medium of the following composition: Dulbecco's modified Eagle medium (DMEM, PanEco, Russia), 10 % fetal bovine serum (FBS, Himedia, India), and 100× penicillin–streptomycin mixture (PanEco, Russia). The medium was changed twice a week. One day before the test, cells were removed from the substrate using 0.25 % trypsin–EDTA solution (Servicebio, China) and seeded into 96-well culture plates at 125000 cells per well. The next day, a suspension of microcrystals at a concentration of 3 μg $mL^{-1}$ in the Cytotox med medium, containing DMEM without phenol red (PanEco, Russia) and 2 % FBS, was added to the cells and they were incubated for 4 h. Lysis of HT-29 by vaterite microcrystals was determined by lactate dihydrogenase (LDG) release using Olvex-LDG kit (Olvex, Russia) and cytotoxicity was calculated in % using Eq. (5):

$$\text{Cytotoxicity} = (A_{\text{exp}} - A_0)/\,(A_{lys} - A_0)\ *\ 100, \tag{5}$$

where $A$ is optical absorbance at 340 nm; lower indices denote: $A_{\text{exp}}$, experimental samples; $A_0$, intact cells, and $A_{lys}$, cells lysed by Triton X-100.

### 2.10. Antioxidant properties of polysaccharides, microcrystals, and biopolymers

Antioxidant properties of the samples were determined using the Fenton reaction with hydroxyl radical detection by luminol chemiluminescence (LCL). To 100 μL of 5–40 μg $mL^{-1}$ microcrystal suspension 17 μM $FeSO_4$ in 0.01 M K-phosphate buffer (pH 7.4) was added and the reaction was initiated by addition of 17 μM $H_2O_2$. The amplitude of the LCL response was measured in control samples without additives and in the presence of 0.8 mg $mL^{-1}$ polysaccharides or particles. Results were presented as the amplitude of the LCL response, % of control.

### 2.11. Iron binding capacity of vaterite microcrystals

The iron binding capacity (IBC) of the samples was determined using the Iron-4-Olvex kit (Olvex, Russia). To 100 μL of a suspension of 5–40 μg $mL^{-1}$ microcrystals 100 μL of 63 μM $FeSO_4$ was added, incubated for 5 min, and centrifuged for 5 min at 5000 rpm. A 40-μL aliquot of supernatant solution was taken from each well of the plate, 200 μL of working reagent was added, incubated for 10 min at 37 °C, and absorbance was measured at 620 nm.

### 2.12. Data processing and statistical analysis

Calculations and statistical processing of the results were performed using Excel, Origin and Statistica 12.0 programs. The results are presented as Mean ± SD, where Mean is arithmetic mean, SD is standard deviation. Statistical significance of differences between groups was assessed using Student's *t*-test for independent variables and Mann–Whitney test. A difference was considered significant at $p < 0.05$.

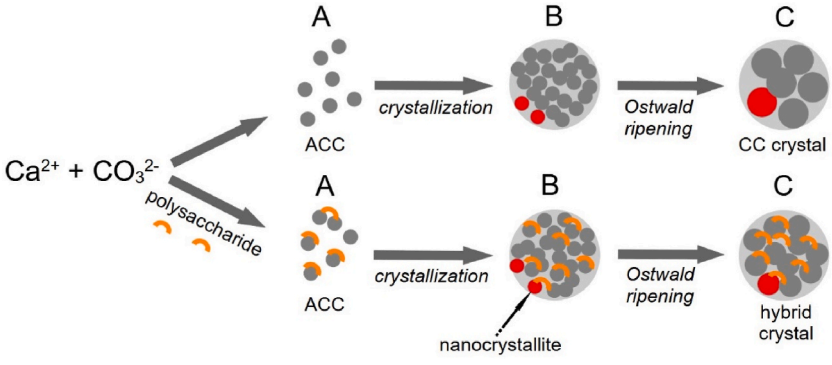


**Fig. 1.** Scheme of the synthesis of CC and hybrid vaterite microcrystals. ACC, amorphous calcium carbonate.

## 3. Results and discussion

### 3.1. Preparation and characterization of hybrid microcrystals

Microcrystals (CC) as well as hybrid microcrystals with polysaccharides with dextran sulfate (CCDS), chondroitin sulfate (CCCS), heparin (CCHE), fucoidan (CCFU), and pectin (CCPE) were obtained by spontaneous crystallization in the absence or presence of biopolymers, respectively (Fig. 1). The yield of microcrystals in three independent cycles of preparation was as follows: for CC 95 ± 6 %, CCDS 96 ± 9 %, CCCS 83 ± 9 %, CCHE 77 ± 9 %, CCFU 85 ± 9 %, CCPE 80 ± 15 %.

The preparation process included: (A) formation of amorphous calcium carbonate; (B) crystallization, and (C) Ostwald maturation of microcrystals, in which the nanocrystallite size changes, followed by washing from unbound polysaccharides and lyophilic drying. The morphology of the formed microcrystals was influenced by the increase in viscosity of the reaction medium due to the presence of biopolymers and the interactions of sulfo- or carboxyl groups of polysaccharides with calcium ions and the formed nanocrystallites [28]. Physicochemical properties of all hybrid and CC microcrystals of vaterite are presented in Table 2.

Using X-ray diffraction analysis (Fig. 1S and Tables 1S and 2), it was found that the crystals were predominantly vaterite, and the proportion of calcite in all samples was less than 3 %. The highest calcite content was observed in CCDS crystals and the lowest, in CCHE. According to energy disperse X-ray spectroscopy data, the presence of sulfur was detected in all hybrid crystals with sulfated polysaccharides (Table 2).

According to the curves obtained using TGA (Fig. 2 A, 2S, Table 2S) the content of each polysaccharide was calculated by mass loss (Fig. 2B–Table 2) owing to thermic decomposition of polymer [23]. The lowest content of polysaccharide of 2 % was registered in CCCS microcrystals, and the highest in CCPE (6.9 %) while other values ranged from 4.7 to 6.0 %. These results are consistent with data of energy disperse X-ray spectroscopy (Table 2) on sulfur in hybrid microcrystals with sulfated polysaccharides, and in CCCS it was the lowest.

According to the electrophoretic laser light scattering data, all used polysaccharides in solutions had negative ζ-potential (Table 3S). Consequently, all hybrid crystals in suspensions had negative ζ-potential (Table 2), which indicated the presence of polyanionic biopolymers on the surface of particles, in contrast to practically uncharged CC with ζ-potential of 2 ± 1 mV.

All hybrid crystals, as well as CC, had a spherical shape according to SEM data, and their diameter varied in the range of 2–4 μm, CC and CCDS were the largest in size (Fig. 3 and S). Most of the CCDS microcrystals had through cracks (Fig. 3 B, H), which could affect their properties. The size of nanocrystallites within the microcrystals ranged from 15 to 46 nm (Table 2). Microcrystals CCDS and CC had the largest nanocrystallite size. CCPE nanocrystallites were the smallest in size, presumably, because of the high viscosity of pectin solution and the formation of its stable gels in the presence of $Ca^{2+}$ ions [61,62]. Nitrogen adsorption/desorption isotherms were obtained on microcrystals (Fig. 3) and the main characteristics of the preparations were determined (Table 2).

Nitrogen adsorption isotherms on CC and hybrid crystals had a hysteresis loop and a convex initial section (Fig. 4), which corresponded to type IV according to the IUPAC classification and indicated the presence of mesopores in the samples under study (Table 2). The hysteresis shape for CCPE belonged to E type, for other hybrid crystals and CC corresponded to mixed type A and E (cylindrical and blind pores). The hybrid crystals had larger pore volume than CC and their surface area increased from CCDS to CCPE (Table 2), while the pore size decreased (Fig. 5), except for CCCS. The smallest pore size and narrowest microcrystal size distribution was observed for CCPE (Fig. 5). The correlation between nanocrystallite size and pore size was found for all hybrid microcrystals (Fig. 4S), except for CCDS, which seems to be due to the presence of a large number of particles with cracks (Fig. 2 B).

We suppose that significant increase in viscosity of the reaction medium could influence the rate of $Ca^{2+}$ diffusion and decreased rate of crystals growth, as it was registered at high concentrations of glycerol or ethylene glycol [63].

Thus, the analysis of physicochemical properties of hybrid vaterite microcrystals obtained by spontaneous crystallization at 5 mg $mL^{-1}$ polysaccharide in the reaction mixture (except for CCDS with cracks) has shown that all microcrystals were characterized by: 1) high content of vaterite; 2) smaller diameter compared to vaterite; 3) smaller diameter of nanocrystallites and of pores, and larger surface area; 4) content of biopolymers of 2–7 %; 5) negative charge unlike vaterite, due to polysaccharide exposure on the surface.

**Table 2**
Physicochemical characteristics of vaterite microcrystals.

| Micro-crystals | Content of calcite, % | Content of poly-saccharide, % | Content of sulfur, % | $D_{crystal}$, μm | $D_{nanocrystalline}$, nm | $S$, $m^2g^{-1}$ | $V_{pores}$, $cm^3g^{-1}$ | $D_{pores}$, nm | ζ-potential, mV |
|---|---|---|---|---|---|---|---|---|---|
| CC | 2.5 | 0 | 0 | 3.6 ± 0.7 | 38 ± 12 | 22 ± 3 | 0.04 | 18.4 | 2 ± 1 |
| CCDS | 2.9 | 6.0 ± 0.3 | 5 | 3.8 ± 0.8 | 46 ± 17 | 37 ± 4 | 0.07 | 5.5 | −13 ± 2 |
| CCCS | 2.6 | 2.0 ± 0.1 | Trace | 1.9 ± 0.5 | 26 ± 12 | 52 ± 5 | 0.12 | 8.5 | −12 ± 2 |
| CCHE | 1.7 | 5.7 ± 0.2 | 5 | 2.0 ± 0.3 | 20 ± 7 | 62 ± 6 | 0.16 | 5.0 | −9 ± 2 |
| CCFU | 2.6 | 4.7 ± 0.2 | 2 | 2.1 ± 0.5 | 18 ± 8 | 60 ± 6 | 0.08 | 3.8 | −12 ± 2 |
| CCPE | 2.0 | 6.9 ± 0.3 | 0 | 2.3 ± 0.7 | 15 ± 4 | 95 ± 10 | 0.08 | 3.4 | −12 ± 2 |

$D_{crystal}$, $D_{nanocrystalline}$, and $D_{pores}$ denote the diameter of crystals, nanocrystallites, and pores, respectively.

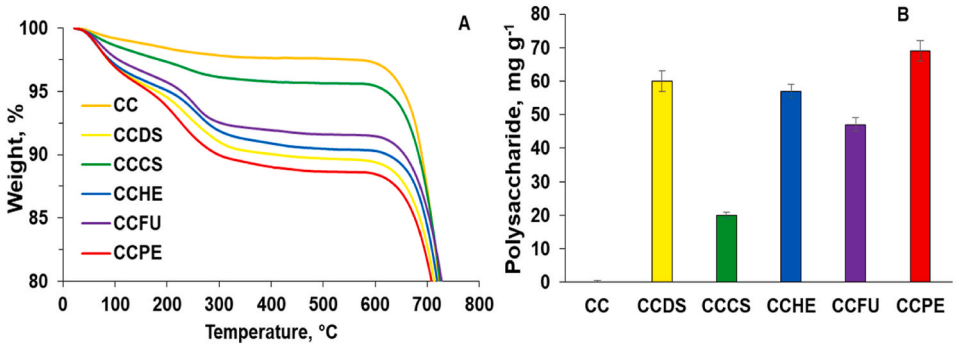


**Fig. 2.** TGA results: TGA curves of control CC and hybrid microcrystals of vaterite (A); content of polysaccharides in microcrystals (B).

**Table 3**
The influence of polysaccharides and vaterite microcrystals on luminol chemiluminescence (LCL) in the Fenton system and the iron binding ability (IBC) of microcrystals.

| Microcrystals | LCL in the Fenton system[a], % | | IBC, nmol μg$^{-1}$ |
|---|---|---|---|
| | Polysaccharide | Microcrystals | Microcrystals |
| CC | – | 115 ± 7 | 0.8 ± 0,1 |
| CCDS | **123 ± 5** | 95 ± 10 | 0.97 ± 0.23 |
| CCCS | 98 ± 2 | 115 ± 7 | 0.69 ± 0.15 |
| CCHE | 98 ± 6 | **75 ± 7**[b] | 0.63 ± 0.15 |
| CCFU | 106 ± 15 | **75 ± 7**[b] | **1.4 ± 0.19**[b] |
| CCPE | 105 ± 7 | 112 ± 10 | 0.8 ± 0.16 |

[a] Effects are presented as a percentage of control values (0.15 M NaCl solution).
[b] The value is significantly different from a respective value for pristine CC, $p < 0.05$.

These results are consistent with earlier published data upon hybrid vaterite microcrystals with heparin (at the same concentration) [23,25], alginate [22], chitosan [19], cellulose [18], mucin [28] and others.

One of the important properties of some polysaccharides is their antioxidant activity towards hydroxyl radical which can non-specifically damage protein, lipid and DNA molecules. Fenton reaction can be used for model studies on hydroxyl radical-scavenging effects of natural biopolymers [64].

In a preliminary study of antioxidant properties in the Fenton system, none of the polysaccharides used at concentrations up to 0.8 mg mL$^{-1}$ inhibited chemiluminescence (LCL), and only for dextran sulfate an increase in the amplitude of the LCL response was observed (Table 3).

The decrease in LCL as compared to the control experiment (0.15 M NaCl solution) was recorded only for CCHE and CCFU microcrystals (up to a concentration of 0.8 mg mL$^{-1}$). Since this effect could be due to both scavenging of hydroxyl radicals and binding of $Fe^{2+}$ ions, IBC of microcrystals was additionally evaluated (Table 3). Only in the case of CCFU microcrystals the IBC increased as compared to CC.

The iron-binding capacity of CCFU microparticles can be attributed to the exposure of fucoidan moieties, according to the data of other researchers [64,65]. Some polysaccharides with chelating ability towards ferrous ions are poor effective hydroxyl radical scavengers [64] while some are hydroxyl radical scavengers with no iron-chelating activity [66]. Chelation of $Fe^{2+}$ ions depends mostly on sulfate groups and their distribution in the molecules [67] while radical scavenging is affected also by monosaccharide composition [68].

Conformation of polysaccharides moieties on the surface of microparticles could favour scavenging of radicals by fucoidan and heparin. They resemble each other in chain structure, but heparin in solution has no iron-chelating and hydroxyl-scavenging activity [69]. It should be noted that not only hydroxyl radicals but also carbonate-anion-radicals are likely formed in Fenton reaction with vaterite microcrystals due to the presence of $HCO_3^-$, at neutral pH values [70]. So, interaction of carbonate anions with polysaccharides [71] is another probable mechanism of radical scavenging by hybrid vaterite microcrystals.

Thus, the nature of the co-precipitated polysaccharide influenced the physicochemical, antioxidant and iron-binding properties of hybrid vaterite crystals.

### *3.2. Study of interaction of protein preparations with hybrid microcrystals*

Negatively charged high-molecular mucin with hydrodynamic diameters of 30–50 nm and 200–300 nm [8], ellipsoid human serum albumin with 3.8 nm and 15 nm diameters [72], catalase of 10 ± 2 nm in diameter, and positively charged chymotrypsin were adsorbed into hybrid microcrystals (Table 4). Negatively charged hybrid microparticles (Table 2) adsorbed a less amount of negatively charged proteins, compared to microcrystals CC with ζ-potential of 2 ± 1 mV, with exception for CCCS with the largest among hybrid

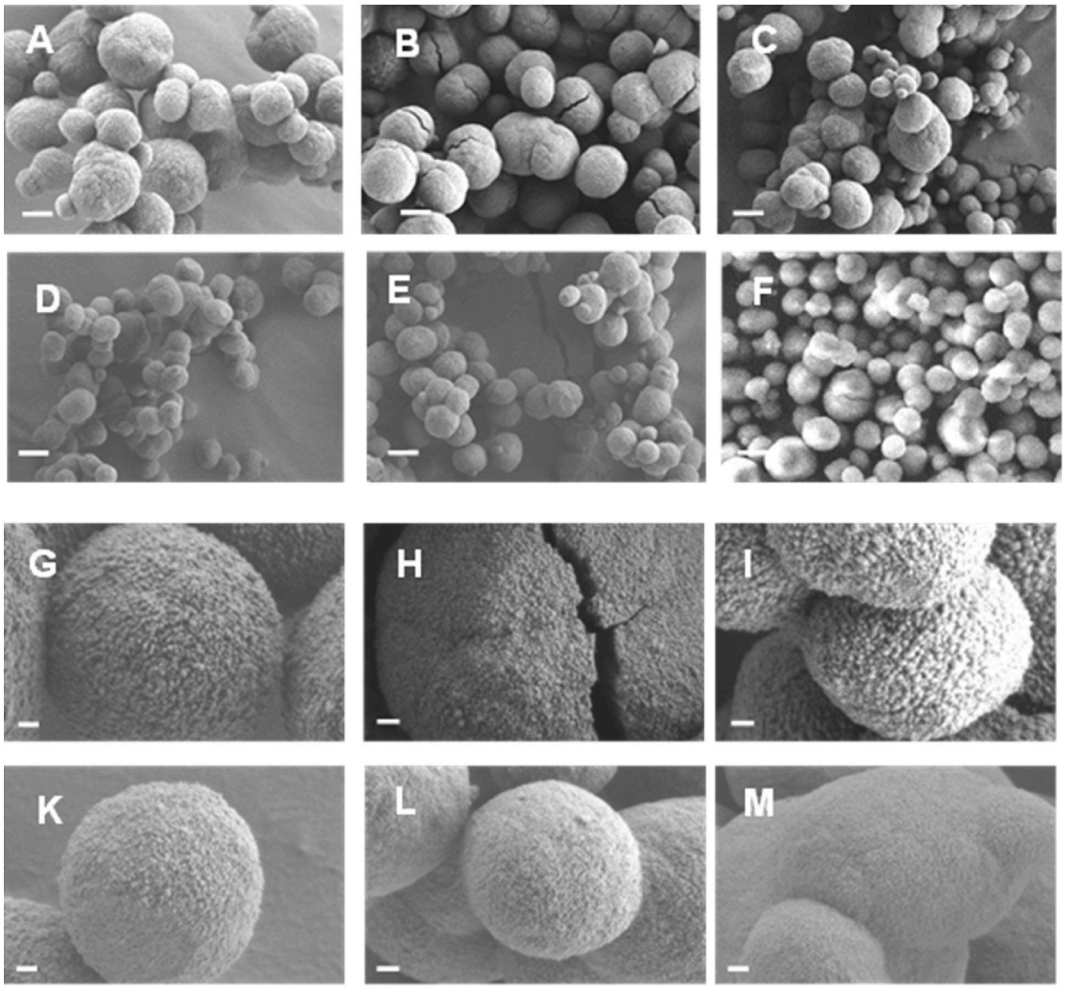


**Fig. 3.** SEM of CC (A, G) and hybrid microcrystals of vaterite with dextran sulfate CCDS (B, H), chondroitin sulfate CCCS (C, I), heparin CCHE (D, K), fucoidan CCFU (E, L), and pectin CCPE (F, M). Scale bar: A–E, 2 μm; G–M, 200 nm.

microparticles pore diameter.

During adsorption of albumin and catalase, a correlation between the pore size of hybrid microcrystals (except for CCDS with cracks) and the amount of incorporated protein was observed (Fig. 5S).

After adsorption of albumin (pI 4.7) which is negatively charged at pH 7, ζ-potential of practically neutral microcrystals CC (Table 4) became negative, while ζ-potential of hybrid vaterite-polysaccharide microparticles remained unchanged. Additional comparison of albumin adsorption isotherms (Table 4S) on CC and CCFU crystals revealed that the maximum adsorption on the hybrid microcrystals was about 2.5 times lower ($q_m$, 5.5 and 13.8 mg $g^{-1}$, respectively), and the value of the inverse of the adsorption equilibrium constant and equal to the polymer concentration at adsorption corresponding to half of $q_m$ was 1.8 times larger ($K_a^{-1}$ is 0.038 and 0.021 mg $mL^{-1}$, respectively).

Sorption of positively charged chymotrypsin with an effective hydrodynamic diameter of 6 ± 1 nm on hybrid crystals of CCCS and CCDS with negative ζ-potential was greater than on practically uncharged CC (Table 4).

Immobilization of proteins should not lead to a decrease in enzyme activity. The specific activity of chymotrypsin sorbed on hybrid crystals of CCCS and CCDS was less than the same value for that sorbed on CC (Table 4). For adsorbed catalase (Table 5), a decrease in the specific activity value of the enzyme relative to control (native enzyme) was observed, similarly to the effect of catalase sorption onto mucin-loaded vaterite [59,60].

The decrease in the activity of enzymes adsorbed on microcrystals may be related to the influence of polysaccharides and to diffusion limitations for substrate and reaction products. Each of these factors was investigated separately. Chondroitin sulfate, heparin, and fucoidan up to a concentration of 5 mg $mL^{-1}$ had no significant effect on enzyme activity in solution (Fig. 6). With increasing dextran sulfate concentration higher than 0.05 mg $mL^{-1}$, an increase in catalase activity was observed. And only at pectin concentration higher than 1 mg $mL^{-1}$ a significant decrease in catalase activity was observed, which is apparently due to the high viscosity of this non-sulfated biopolymer.

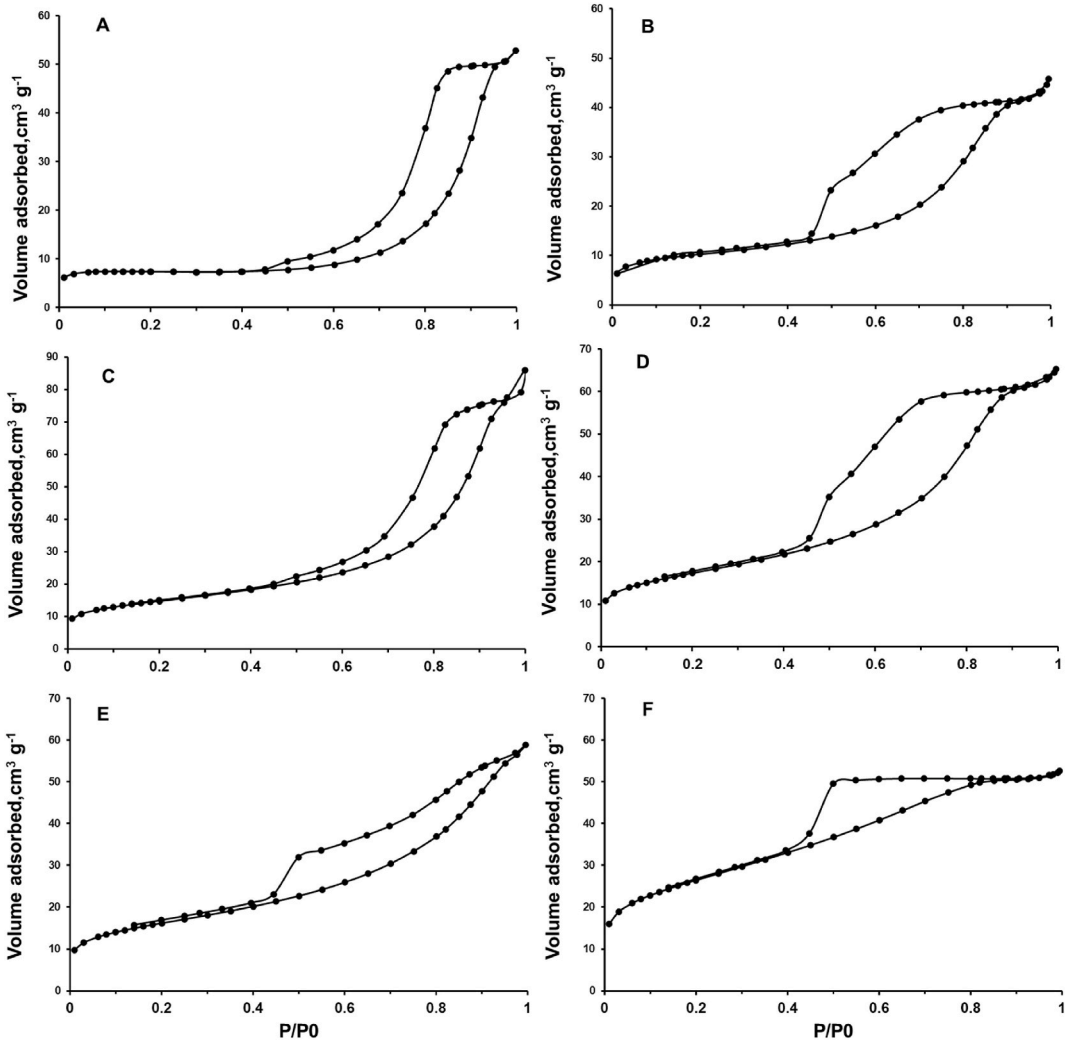


**Fig. 4.** Nitrogen adsorption/desorption isotherms on CC (A) and hybrid microcrystals of vaterite with dextran sulfate CCDS (B), chondroitin sulfate CCCS (C), heparin CCHE (D), fucoidan CCFU (E), and pectin CCPE (F).

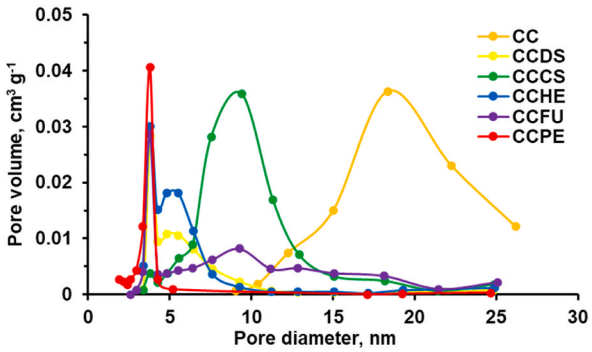


**Fig. 5.** Pore distributions in microcrystals according to the Barrett–Joyner–Halenda method.

The study of the effect of hydrogen peroxide concentration on the rate of its decomposition by catalase adsorbed on hybrid microcrystals (Fig. 6S) has shown that the catalytic constant ($k_{cat} = V_{max}/E_o$), calculated from the content of active centers of the enzyme, is lower than that of native (dissolved) catalase, but higher than that of catalase adsorbed on pristine CC crystals (Table 5). The

**Table 4**
The adsorption of drugs on microcrystals.

| Micro-crystals | $q_e$, mg g$^{-1}$ | | | | ζ-Potential of crystals after inclusion of albumin, mV | Chymo-trypsin activity, % |
|---|---|---|---|---|---|---|
| | Mucin, 600 kDa, pI 3–4, 30 - 50 and 200–300 nm | Albumin, 68 kDa, pI 4.7, 3.8x15 nm | Catalase, 250 kDa, pI 5.4, 10.5 nm | Chymotrypsin, 25 kDa, pI 8.8, 4 - 7 нМ | | |
| CC | **7 ± 2** | **14 ± 2** | **19 ± 5** | 4 ± 2 | **−19 ± 2** | 156 ± 24 |
| CCDS | 1 ± 1 | 12 ± 3 | 15 ± 4 | **16 ± 5** | −12 ± 12 | 69 ± 10 |
| CCCS | **8 ± 2** | **13 ± 2** | **18 ± 5** | 8 ± 3 | −12 ± 1 | 137 ± 22 |
| CCHE | 2 ± 1 | 11 ± 2 | 11 ± 3 | n.d. | −10 ± 1 | n.d. |
| CCFU | 3 ± 1 | 7 ± 1 | 4 ± 1 | n.d. | −10 ± 1 | n.d. |
| CCPE | 4 ± 1 | 8 ± 1 | 8 ± 2 | n.d. | −11 ± 1 | n.d. |

**Table 5**
Catalase immobilization on the microcrystals. The adsorption is performed in 0.05 M Tris buffer pH 7.0 followed by washing twice at 25 °C.

| Sample | Catalase activity, U mg$^{-1}$ protein | $K_m$, mM | $k_{cat}$•10$^{-7}$, s$^{-1}$ |
|---|---|---|---|
| Catalase | 1239 ± 149 | 74 ± 33 | 5.6 ± 2.4 |
| CC | 515 ± 62 | 4 ± 1 | 0.7 ± 0.2 |
| CCDS | 521 ± 61 | 15 ± 6 | **4.2 ± 2.4** |
| CCCS | 539 ± 65 | 16 ± 7 | 2.7 ± 0,9 |
| CCHE | 466 ± 56 | 23 ± 6 | 4.7 ± 1.9 |
| CCFU | **876 ± 105** | 5 ± 2 | **3.9 ± 1.5** |
| CCPE | **728 ± 109** | 2.0 ± 0.3 | 2.7 ± 0.2 |

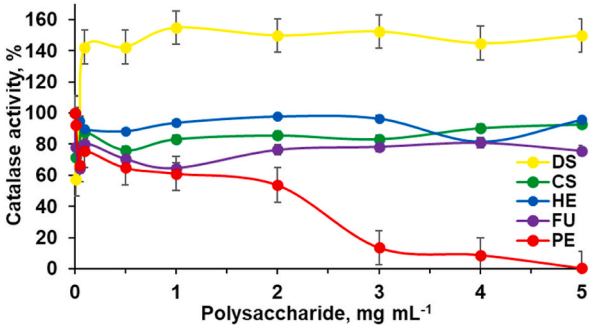


**Fig. 6.** Dose dependence of the effect of polysaccharides on catalase activity in solution. Conditions: 0.05 M Tris buffer, pH 7.0, 25°C.

decrease in $k_{cat}$ indicated the presence of diffusion difficulties for the substrate in the microcrystals compared to the dissolved enzyme, but the Michaelis constant $K_m$ for the adsorbed catalase also decreased. It should be noted that an objective assessment of the decrease in $K_m$ is difficult due to the irreversibility of the first stage of hydrogen peroxide decomposition by catalase (see Eqs. (1S) and (2S)). Additionally, using CCDS as an example, we demonstrated that enzyme activity decreased with increasing amount of adsorbed catalase, which presumably was/could be associated with steric hindrance (Table 5S).

Our hypothesis was that cationic proteins should be loaded into hybrid microcrystals with anionic polysaccharides better than anionic ones. In fact, hybrid microcrystals with polysaccharides are designed in order to increase their loading capacity for cationic proteins which are poorly adsorbed by vaterite microcrystals [17]. In the current study we have confirmed this hypothesis by the data on positively-charged chymotrypsin adsorption: it increased with CCDS and CCCS compared to CC, unlike sorption of negatively charged proteins (Table 4).

Proteins which have negative charge at pH over pI value nevertheless have some positively charged sites capable to interact with negatively charged sites in polysaccharides. As we have shown earlier on the example of catalase, if the pore size is comparable to the size of protein molecules, its penetration inside CC microcrystals is observed [17], while if it is smaller, protein sorption occurs on the surface of microcrystals [59]. Both hydrogen and hydrophobic interactions can play an important role here as we have shown for hybrid mucin-vaterite microparticles [28].

Non-proteinaceous drugs can be also successfully loaded into hybrid microcrystals of vaterite with biopolymers via co-precipitation or sorption, as we have shown earlier for anticancer anthracycline class medication doxorubicin (544 Da, pKa 8.6). The co-loading of

mucin and doxorubicin into microcrystals of vaterite significantly improved inclusion of the drug and its prolonged release [28].

We did not study proteolytic degradation of the proteins adsorbed on the hybrid microcrystals in the current research, but we suppose that polysaccharides exposed on the surface would sterically hinder the contact of the proteases with adsorbed proteins. Earlier we have studied proteolysis of catalase adsorbed on mucin-vaterite hybrid microcrystals [59] and found that incorporation of mucin resulted in drop in pore size to 8 nm, shift of the surface charge to −7 mV and stabilization of catalase upon lyophilisation and storage compared to catalase adsorbed on vaterite (CC). Treatment of microcrystals for 3 h with trypsin decreased activity of catalase adsorbed on mucin-vaterite microcrystals to 60 % while activity of catalase in solution or loaded into CC microparticles was no more than 40 % of initial values.

Thus, the study of adsorption on hybrid microcrystals with polysaccharides revealed a greater inclusion of positively charged chymotrypsin, as well as a decrease in the inclusion of negatively charged albumin, catalase, and mucin with a decrease in the pore diameter of the crystals. For catalase adsorbed on CC and hybrid microcrystals, a protein concentration-dependent decrease in specific activity relative to native enzyme was observed, as well as a decrease in $K_m$ and $k_{cat}$, which suggests possible advantageousness of the inclusion of an antioxidant enzyme for local delivery to inflammation foci. Mucin adsorption on all tested hybrid microcrystals, except for CCCS with the largest pore size, decreased relative to CC microcrystals.

### 3.3. Study of biocompatibility of hybrid microcrystals

Micro particulate carriers are found to have lots of applications in inflammatory bowel diseases patients [73,74]. Pectin [75] and fucoidan [76] showed protective effects in bowel diseases. Vaterite is biocompatible and biodegradable and its's worth mentioning that calcium may have a prebiotic effect [77]. Incorporation of polysaccharides can significantly influence properties of vaterite microcrystals.

Biocompatibility of microcrystals depends on their ability to damage the cell membrane through direct physicochemical interactions or cellular reactions to the particles, including those mediated by proteins of the biological medium (e.g., blood plasma).

Polysaccharides included in microcrystals may have a nonspecific effect by shielding the vaterite surface and thus preventing protein adsorption or crystal–cell interactions. On the other hand, polysaccharides exposed on the surface of hybrid microcrystals may retain their own specific biological activity. In terms of blood biocompatibility, interaction between microparticles and blood cells could induce membrane damage while protein adsorption can be followed by activation of coagulation cascade and formation of blood clot. To characterize the potential biological effects due to the presence of polysaccharides, we analyzed the effects of hybrid microcrystals on blood plasma coagulation in vitro and on adenosine diphosphate (ADP)-induced platelet aggregation in rabbit PRP. To assess cytotoxicity, a hemolysis model was used.

Under conditions of standard contact (kaolin) and phospholipid (kefalin) activation of plasma coagulation, microcrystals of CC, CCCS, and CCPE (0.5 mg mL$^{-1}$) slightly increased the APTT, while CCDS, CCHE, and CCFU increased the clotting time about 10-fold (Fig. 7A). This means that they are effective inhibitors of factors of the intrinsic coagulation mechanism (factors XII, XI, IX, or VIII).

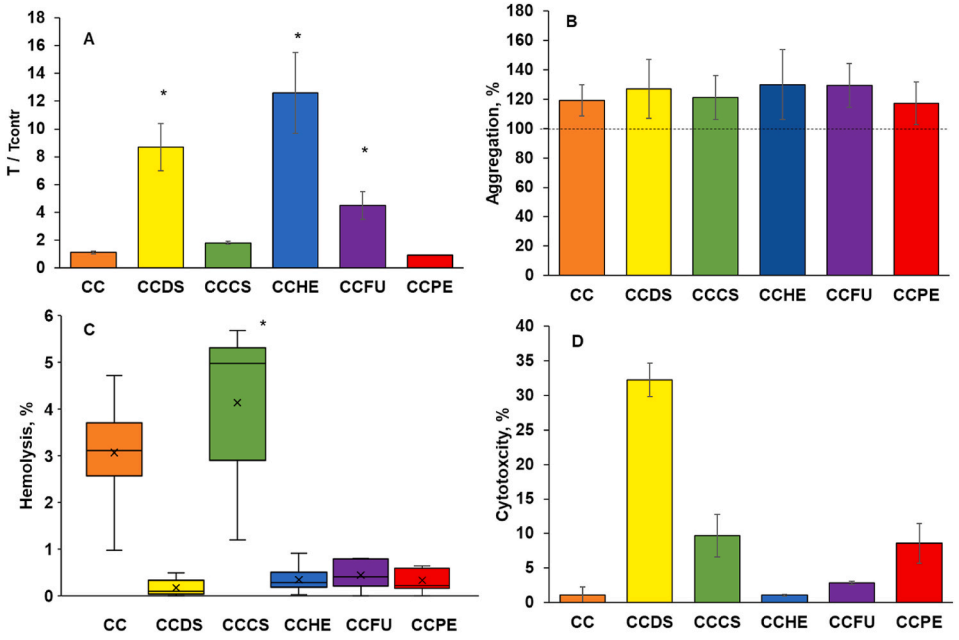


**Fig. 7.** Effect of microcrystals on (A) plasma coagulation as assessed by the estimation of APTT at 0.5 mg mL$^{-1}$ particles in the sample (control values, 20 s); (B) ADP-induced platelet aggregation in rabbit PRP (0. 5 mg mL$^{-1}$ particles in the sample); (C) erythrocyte lysis (3.3 mg mL$^{-1}$ particles, 2 h), and (D) LDH release by HT-29 cells (3 mg mL$^{-1}$ particles, $10^5$ cells, 4 h).

These results are supported by literature data on the anticoagulant activity of sulfated dextran sulfate [78], heparin and fucoidan [79]. Indeed, fucoidan is considered as an alternative anticoagulant without the hemorrhage drawback compared to heparin [80].

When CC and all hybrid microcrystals were added at the same concentration as in the APTT test (0.5 mg $mL^{-1}$) to rabbit PRP, no change in light transmission corresponding to a change in the degree of ADP-induced cell aggregation was observed (Fig. 7B).

Negatively charged hybrid microcrystals CCDS, CCHE, CCFU, and CCPE induced less erythrocyte lysis compared with control CC and hybrid CCCS, which had the largest pore size (Fig. 7C–Table 2). The increase in hemolytic activity of CCCS microcrystals compared to CC may be due to increased erythrocyte adhesion in the presence of chondroitin sulfate [80]. These data show low non-specific cytotoxicity of native and hybrid vaterite microcrystals towards cellular membrane but the specific effects of some polysaccharides should be taken in account as was shown for CS.

Moreover, effects of microcrystals can be significantly influenced by the adsorption of the biological fluid components [81,82]. Assayed in our research mucin-binding capacity of microcrystals (Table 4) witnesses their potential mucosal biocompatibility [83].

The damage to HT-29 cell membranes was assessed by the activity of released LDH (Fig. 7D). Microcrystals of CC, as well as CCHE with the lowest negative charge modulus did not cause cell membrane damage, whereas CCCS, CCFU, and CCPE increased LDH release by no more than 10 %. Also, in experiments with HeLa cells porous spherical $CaCO_3$ microcrystals had only a little cytotoxicity: even at the concentration of 400 μg $mL^{-1}$, the viabilities of the treated cells were 89.6 % [84]. Only microcrystals of CCDS had the greater cytolytic effect, which is consistent with the data on the toxicity of dextran sulfate to intestinal epithelial cells [85].

Thus, it was shown for the first time that the presence of co-precipitated natural polysaccharides in hybrid microcrystals of vaterite significantly changes the nature and degree of cellular responses in vitro. Moreover, modification of vaterite with fucoidan rendered microcrystals both iron-chelating and hydroxyl-scavenging, and these antioxidant effects can be enhanced via sorption of antioxidant enzymes such as catalase.

## 4. Conclusions

In this work, the properties of hybrid microcrystals of vaterite with natural polysaccharides from different sources (sulfated dextran sulfate, chondroitin sulfate, heparin, fucoidan and non-sulfated pectin) were investigated, which due to the presence of antioxidant, anti-inflammatory, immunomodulatory and anticancer properties (Table 1) are of interest for the development of drug delivery carriers.

The results obtained in this work show that co-precipitation of polysaccharides into vaterite microcrystals can be used to modify their properties. The incorporation of polysaccharides into hybrid microcrystals allows us to vary their morphology (pore and nanocrystallite diameter, surface area, pore volume) and change the ζ-potential of the surface (Table 2). Due to these features, hybrid microcrystals acquire the ability to interact differently with proteins depending on the molecule size and charge of the latter (Table 4). This is demonstrated both with respect to adsorption of target proteins, as exemplified by enzymes catalase and chymotrypsin, and with respect to components of biological media such as blood plasma albumin and mucin, which is the major glycoprotein of the mucus.

The nature of the incorporated polysaccharide significantly affects the enzyme activity in solution and during adsorption on the hybrid microcrystals; however, no complete loss of enzyme activity was observed for any of the crystals studied (Tables 4 and 5). In contrast, an increase in the specific activity of adsorbed catalase was found for hybrid microcrystals with pectin CCPE and fucoidan CCFU as compared to CC microcrystals. (Table 5).

Co-precipitation with polysaccharides can influence the antioxidant properties of hybrid microcrystals (Table 3) and modulate their effects on the proteins and cells (Fig. 7). An anticoagulant effect was observed for microcrystals with heparin CCHE, fucoidan CCFU, and dextran sulfate CCDS (Fig. 7A). Only microcrystals with dextran sulfate CCDS showed a pronounced cytotoxic effect against HT-29 cells (Fig. 7D) unlike other microcrystals. Co-precipitation of polysaccharides did not increase the nonspecific cytotoxicity of hybrid microcrystals towards red blood cells (Fig. 7C) and platelets (Fig. 7B).

Taken together, the results obtained show the possibility of creating polyfunctional hybrid microcrystals of vaterite by modifying them with polysaccharides and incorporating target proteins, including those with enzymatic activity. The use of polysaccharides of different nature allows optimizing the biocompatibility of the hybrid vaterite microcrystals.

Incorporation of therapeutically important proteins and enzymes into cheap hybrid microcrystals of vaterite with polysaccharides is important for the development of new delivery vehicles, and further obtaining of crystals with polysaccharides of nano size can open additional areas of their use.

## Data availability

The raw/processed data required to reproduce these findings cannot be shared at this time due to technical or time limitations.

## Ethics declaration

Blood samples were withdrawn from healthy volunteers with their informed consent, in accordance with the protocol approved by the ethical committee of Lopukhin Federal Research and Clinical Center of Physical-Chemical Medicine (protocol No. 2022/10/05).

Rabbit blood was withdrawn according to protocol approved by the ethical committee of Lopukhin Federal Research and Clinical Center of Physical-Chemical Medicine (Protocol No. 2022/10/05-1).

## CRediT authorship contribution statement

**Nadezhda G. Balabushevich:** Writing – review & editing, Writing – original draft, Supervision, Project administration, Conceptualization. **Liliya N. Maltseva:** Methodology, Formal analysis. **Lyubov Y. Filatova:** Writing – review & editing, Methodology, Formal analysis. **Daniil V. Mosievich:** Methodology, Formal analysis. **Pavel I. Mishin:** Methodology, Formal analysis. **Margarita E. Bogomiakova:** Writing – review & editing, Writing – original draft, Methodology, Investigation, Formal analysis, Data curation. **Olga S. Lebedeva:** Writing – review & editing, Writing – original draft, Methodology, Investigation, Formal analysis, Data curation. **Marina A. Murina:** Writing – review & editing, Writing – original draft, Methodology, Investigation, Formal analysis, Data curation. **Dmitry V. Klinov:** Methodology, Formal analysis. **Ekaterina A. Obraztsova:** Methodology, Formal analysis. **Zaira F. Kharaeva:** Methodology, Formal analysis. **Roxalana K. Firova:** Methodology, Formal analysis. **Daria V. Grigorieva:** Methodology, Formal analysis. **Irina V. Gorudko:** Methodology, Formal analysis. **Oleg M. Panasenko:** Writing – review & editing, Writing – original draft, Supervision, Resources, Funding acquisition, Formal analysis. **Elena V. Mikhalchik:** Writing – review & editing, Writing – original draft, Project administration, Methodology, Investigation, Data curation, Conceptualization.

## Declaration of competing interest

The authors declare the following financial interests/personal relationships which may be considered as potential competing interests:Panasenko O.M. reports financial support was provided by Russian Science Foundation (project No. 23-45-10026). Gorudko I reports financial support was provided by Belarusian Republican Foundation for Basic Research (project No. B23RNF-093). If there are other authors, they declare that they have no known competing financial interests or personal relationships that could have appeared to influence the work reported in this paper.

## Acknowledgements

This research was funded by a joint grant from the Russian Science Foundation (project No. 23-45-10026) and the Belarusian Republican Foundation for Basic Research (project No. B23RNF-093), and the synthesis of microparticles was carried out for the purpose of the registration theme No. 121041500039-8 and with the use of devices purchased according to the Development Program of Lomonosov Moscow State University.

## Appendix A. Supplementary data

Supplementary data to this article can be found online at https://doi.org/10.1016/j.heliyon.2024.e33801.

## References

[1] D.B. Trushina, T.N. Borodina, S. Belyakov, M.N. Antipin, Calcium carbonate vaterite particles for drug delivery: Advances and challenges, Mater. Today Adv. 14 (2022) 100214, https://doi.org/10.1016/j.mtadv.2022.100214.
[2] A. Vikulina, D. Voronin, R. Fakhrullin, V. Vinokurov, D. Volodkin, Naturally derived nano- and micro- drug delivery vehicles: halloysite, vaterite and nanocellulose, New J. Chem. 44 (2020) 5638–5655, https://doi.org/10.1016/j.mtadv.2022.100214.
[3] A.D. Trofimov, A.A. Ivanova, M.V. Zyuzin, A.S. Timin, Porous inorganic carriers based on silica, calcium carbonate and calcium phosphate for controlled/modulated drug delivery: fresh outlook and future perspectives, Pharmaceutics 10 (2018) 167, https://doi.org/10.3390/pharmaceutics10040167.
[4] V.K.K. Paravastu, S.R. Yarraguntla, A. Suvvari, Role of nanocomposites in drug delivery, GSC Biol, Pharm. Sci. 8 (2019) 94–103, https://doi.org/10.30574/gscbps.2019.8.3.0150.
[5] G. Cavallaro, G. Lazzara, R. Fakhrullin, Mesoporous inorganic nanoscale particles for drug adsorption and controlled release, Ther. Deliv. 9 (2018) 287–301, https://doi.org/10.4155/tde-2017-0120.
[6] A. Vikulina, J. Webster, D. Voronin, E. Ivanov, R. Fakhrullin, V. Vinokurov, D. Volodkin, Mesoporous additive-free vaterite $CaCO_3$ crystals of untypical sizes: from submicron to Giant, Mater. Des. 197 (2021) 109220, https://doi.org/10.1016/j.matdes.2020.109220.
[7] S. Maleki Dizaj, S. Sharifi, E. Ahmadian, A. Eftekhari, K. Adibkia, F. Lotfipour, An update on calcium carbonate nanoparticles as cancer drug/gene delivery system, Expet Opin. Drug Deliv. 16 (2019) 331–345, https://doi.org/10.1080/17425247.2019.1587408.
[8] Y. Zhao, Z. Luo, M. Li, Q. Qu, X. Ma, S.H. Yu, Y. Zhao, A preloaded amorphous calcium carbonate/doxorubicin@silica nanoreactor for pH-responsive delivery of an anticancer drug, Angew. Chem. Int. Ed. Engl. 54 (2015) 919–922, https://doi.org/10.1002/anie.201408510.
[9] N.G. Balabushevich, E.A. Kovalenko, E.V. Mikhalchik, L.Y. Filatova, D. Volodkin, A.S. Vikulina, Mucin adsorption on vaterite $CaCO_3$ microcrystals for the prediction of mucoadhesive properties, J. Colloid Interface Sci. 545 (2019) 330–339, https://doi.org/10.1016/j.jcis.2019.03.042.
[10] N.G. Balabushevich, E.A. Sholina, E.V. Mikhalchik, L.Y. Filatova, A.S. Vikulina, D. Volodkin, Self-assembled mucin-containing microcarriers via hard templating on $CaCO_3$, crystals, Micromachines 9 (2018) 307, https://doi.org/10.3390/mi9060307.
[11] Y. Svenskaya, T. Pallaeva, Exploiting benefits of vaterite metastability to design degradable systems for biomedical applications, Pharmaceutics 15 (2023) 2574, https://doi.org/10.3390/pharmaceutics15112574.
[12] I. Marchenko, T. Borodina, D. Trushina, I. Rassokhina, Y. Volkova, V. Shirinian, I. Zavarzin, A. Gogin, T. Bukreeva, Mesoporous particle-based microcontainers for intranasal delivery of imidazopyridine drugs, J. Microencapsul. 35 (2018) 657–666, https://doi.org/10.1080/02652048.2019.1571642.
[13] O. Gusliakova, E.N. Atochina-Vasserman, O. Sindeeva, S. Sindeev, S. Pinyaev, N. Pyataev, V. Revin, G.B. Sukhorukov, D. Gorin, A.J. Gow, Use of submicron vaterite particles serves as an effective delivery vehicle to the respiratory portion of the lung, Front. Pharmacol. 9 (2018) 559, https://doi.org/10.3389/fphar.2018.00559.
[14] D. Liu, G. Jiang, W. Yu, L. Li, Z. Tong, X. Kong, J. Yao, Oral delivery of insulin using $CaCO_3$-based composite nanocarriers with hyaluronic acid coatings, Mater. Lett. 188 (2017) 263–266, https://doi.org/10.1016/j.matlet.2016.10.117.

[15] P.V. Binevski, N.G. Balabushevich, V.I. Uvarova, A.S. Vikulina, D. Volodkin, Bio-friendly encapsulation of superoxide dismutase into vaterite $CaCO_3$ crystals. Enzyme activity, release mechanism, and perspectives for ophthalmology, Colloids Surf. B Biointerfaces 181 (2019) 437–449, https://doi.org/10.1016/j.colsurfb.2019.05.077.

[16] D. Volodkin, $CaCO_3$ templated micro-beads and -capsules for bioapplications, Adv. Colloid Interface Sci. 207 (2014) 306–324, https://doi.org/10.1016/j.cis.2014.04.001.

[17] N.G. Balabushevich, A.V. Lopez de Guerenu, N.A. Feoktistova, D. Volodkin, Protein loading into porous $CaCO_3$ microspheres: adsorption equilibrium and bioactivity retention, Phys. Chem. Chem. Phys. 17 (2015) 2523–2530, https://doi.org/10.1039/c4cp04567j.

[18] L.H. Fu, C. Qi, Y.R. Hu, C.G. Mei, M.G. Ma, Cellulose/vaterite nanocomposites: sonochemical synthesis, characterization, and their application in protein adsorption, Mater. Sci. Eng. C Mater. Biol. Appl. 96 (2019) 426–435, https://doi.org/10.1016/j.msec.2018.11.061.

[19] J.H. Byeon, Photo-derived transformation from modified chitosan@calcium carbonate nanohybrids to nanosponges, Sci. Rep. 6 (2016) 28782, https://doi.org/10.1038/srep28782. PMID: 27338869.

[20] H.C. Dang, X. Yuan, Q. Xiao, W.-X. Xiao, Y.-K. Luo, X.-L. Wang, F. Song, Y.-Z. Wang, Facile batch synthesis of porous vaterite microspheres for high efficient and fast removal of toxic heavy metal ions, J. Environmental. Chem. Eng. 5 (2017) 4505–4515, https://doi.org/10.1016/j.jece.2017.08.029.

[21] J. Wang, J.-S. Chen, J.-Y. Zong, D. Zhao, F. Li, R.-X. Zhuo, S.-X. Cheng, Calcium carbonate/carboxymethyl chitosan hybrid microspheres and nanospheres for drug delivery, J. Phys. Chem. C 114 (2010) 18940–18945, https://doi.org/10.1021/jp105906p.

[22] G.A. Islan, M.L. Cacicedo, V.E. Bosio, G.R. Castro, Development and characterization of new enzymatic modified hybrid calcium carbonate microparticles to obtain nano-architectured surfaces for enhanced drug loading, J. Colloid Interface Sci. 439 (2015) 76–87, https://doi.org/10.1016/j.jcis.2014.10.007.

[23] P. Shi, S. Luo, B. Voit, D. Appelhans, X. Zan, A facile and efficient strategy to encapsulate the model basic protein lysozyme into porous $CaCO_3$, J. Mater. Chem. B 6 (2018) 4205–4215, https://doi.org/10.1039/c8tb00312b.

[24] P. Shi, J. Qin, J. Hu, Y. Bai, X. Zan, Insight into the mechanism and factors on encapsulating basic model protein, lysozyme, into heparin doped $CaCO_3$, Colloid. Surf. B: Biointerfaces 175 (2019) 184–194, https://doi.org/10.1016/j.colsurfb.2018.11.079.

[25] N. Sudareva, O. Suvorova, N. Saprykina, N. Smirnova, P. Bel'tyukov, S. Petunov, A. Radilov, A. Vilesov, Two-level delivery systems based on $CaCO_3$ cores for oral administration of therapeutic peptide, J. Microencapsul. 35 (2018) 619–634, https://doi.org/10.1080/02652048.2018.1559247.

[26] N.N. Sudareva, O.M. Suvorova, D.N. Suslov, O.V. Galibin, A.D. Vilesov, Dextran sulfate coated $CaCO_3$ vaterites as the systems for regional administration of doxorubicin to rats, Cell Ther. Transplant 10 (2021) 71–76, https://doi.org/10.18620/ctt-1866-8836-2021-10-3-4-71-77.

[27] M. Mihai, C. Steinbach, M. Aflori, S. Schwarz, Design of high sorbent pectin/$CaCO_3$ composites tuned by pectin characteristics and carbonate source, Mater. Des. 86 (2015) 388–396, https://doi.org/10.1016/j.matdes.2015.07.088.

[28] N.G. Balabushevich, E.A. Kovalenko, I.M. Le-Deygen, L.Y. Filatova, D. Volodkin, A.S. Vikulina, Hybrid $CaCO_3$–mucin crystals: effective approach for loading and controlled release of cationic drugs, Mater. Des. 182 (2019) 108020, https://doi.org/10.1016/j.matdes.2019.108020.

[29] B.S. Paliya, V.K. Sharma, M. Sharma, D. Diwan, Q.D. Nguyen, T.M. Aminabhavi, G. Rajauria, B.N. Singh, V.K. Gupta, Protein–polysaccharide nanoconjugates: potential tools for delivery of plant-derived nutraceuticals, Food Chem. 428 (2023) 136709, https://doi.org/10.1016/j.foodchem.2023.136709.

[30] N.N. Drozd, Y.S. Logvinova, M.A. Torlopov, E.V. Udoratina, Effect of sulfation and molecular weight on anticoagulant activity of dextran, Bull. Exp. Biol. Med. 162 (2017) 462–465, https://doi.org/10.1007/s10517-017-3640-2.

[31] S. Andreu, C. von Kobbe, P. Delgado, I. Ripa, M.J. Buzón, M. Genescà, N. Gironès, J. Del Moral-Salmoral, G.A. Ramírez, S. Zúñiga, L. Enjuanes, J.A. López-Guerrero, R. Bello-Morales, Dextran sulfate from *Leuconostoc mesenteroides* B512F exerts potent antiviral activity against SARS-CoV-2 *in vitro* and *in vivo*, Front. Microbiol. 14 (2023) 1185504, https://doi.org/10.3389/fmicb.2023.1185504.

[32] Y. Hori, J. Hoshino, C. Yamazaki, T. Sekiguchi, S. Miyauchi, K. Horie, Effects of chondroitin sulfate on colitis induced by dextran sulfate sodium in rats, Jpn. J. Pharmacol. 85 (2001) 155–160, https://doi.org/10.1254/jjp.85.155.

[33] G.M. Campo, A. Avenoso, S. Campo, A.M. Ferlazzo, A. Calatroni, Antioxidant activity of chondroitin sulfate, Adv. Pharmacol. 53 (2006) 417–431, https://doi.org/10.1016/S1054-3589(05)53020-5.

[34] A. Rani, R. Baruah, A. Goyal, Physicochemical, antioxidant and biocompatible properties of chondroitin sulphate isolated from chicken keel bone for potential biomedical applications, Carbohydr. Polym. 159 (2017) 11–19, https://doi.org/10.1016/j.carbpol.2016.12.015.

[35] S. Sakai, H. Akiyama, Y. Sato, Y. Yoshioka, R.J. Linhardt, Y. Goda, T. Maitani, T. Toida, Chondroitin sulfate intake inhibits the IgE-mediated allergic response by down-regulating Th2 responses in mice, J. Biol. Chem. 281 (2006) 19872–19880, https://doi.org/10.1074/jbc.M509058200.

[36] Y. Wang, Y. Zhang, P. Wang, T. Jing, Y. Hu, X. Chen, Research progress on antiviral activity of heparin, Curr. Med. Chem. 31 (2024) 7–24, https://doi.org/10.2174/0929867330666230203124032.

[37] D. Grant, W.F. Long, G. Mackintosh, F.B. Williamson, The antioxidant activity of heparins, Biochem. Soc. Trans. 24 (1996) 194S, https://doi.org/10.1042/bst024194.

[38] T. Ahmed, J. Garrigo, I. Danta, Preventing bronchoconstriction in exercise-induced asthma with inhaled heparin, N. Engl. J. Med. 329 (1993) 90–95, https://doi.org/10.1056/NEJM199307083290204.

[39] M. Kragh, L. Binderup, P.J. Vig Hjarnaa, E. Bramm, K.B. Johansen, C. Frimundt Petersen, Non-anti-coagulant heparin inhibits metastasis but not primary tumor growth, Oncol. Rep. 14 (2005) 99–104, https://doi.org/10.3892/or.14.1.99.

[40] A. Husni, N. Izmi, F.Z. Ayunani, A. Kartini, N. Husnayain, A. Isnansetyo, Characteristics and antioxidant activity of fucoidan from *Sargassum hystrix*: effect of extraction method, Int. J. Food Sci. 2022 (2022) 3689724, https://doi.org/10.1155/2022/3689724.

[41] L. Wang, T.U. Jayawardena, H.W. Yang, H.G. Lee, M.C. Kang, K.K.A. Sanjeewa, J.Y. Oh, Y.J. Jeon, Isolation, characterization, and antioxidant activity evaluation of a fucoidan from an enzymatic digest of the edible seaweed, *Hizikia fusiforme*, Antioxidants 9 (2020) 363, https://doi.org/10.3390/antiox9050363.

[42] S. Luthuli, S. Wu, Y. Cheng, X. Zheng, M. Wu, H. Tong, Therapeutic effects of fucoidan: a review on recent studies, Mar. Drugs 17 (2019) 487, https://doi.org/10.3390/md17090487.

[43] B. Pradhan, R. Nayak, S. Patra, P.P. Bhuyan, P.K. Behera, A.K. Mandal, C. Behera, J.S. Ki, S.P. Adhikary, D. MubarakAli, M. Jena, A state-of-the-art review on fucoidan as an antiviral agent to combat viral infections, Carbohydr. Polym. 291 (2022) 119551, https://doi.org/10.1016/j.carbpol.2022.119551.

[44] G. van Weelden, M. Bobiński, K. Okła, W.J. van Weelden, A. Romano, J.M.A. Pijnenborg, Fucoidan structure and activity in relation to anti-cancer mechanisms, Mar. Drugs 17 (2019) 32, https://doi.org/10.3390/md17010032.

[45] N. Wathoni, C. Yuan Shan, W. Yi Shan, T. Rostinawati, R.B. Indradi, R. Pratiwi, M. Muchtaridi, Characterization and antioxidant activity of pectin from Indonesian mangosteen (Garcinia mangostana L.) rind, Heliyon 5 (2019) e02299, https://doi.org/10.1016/j.heliyon.2019.e02299.

[46] L.M. Vogt, N.M. Sahasrabudhe, U. Ramasamy, D. Meyer, G. Pullens, M.M. Faas, K. Venema, H.A. Schols, P. de Vos, The impact of lemon pectin characteristics on TLR activation and T84 intestinal epithelial cell barrier function, J. Funct.Foods 22 (2016) 398–407, https://doi.org/10.1016/j.jff.2016.02.002.

[47] J.H. Lee, Y.K. Lee, Y.R. Choi, J. Park, S.K. Jung, Y.H. Chang, The characterization, selenylation and anti-inflammatory activity of pectic polysaccharides extracted from Ulmus pumila L, Int. J. Biol. Macromol. 111 (2018) 311–318, https://doi.org/10.1016/j.ijbiomac.2018.01.005.

[48] A. Delvart, C. Moreau, B. Cathala, Dextrans and dextran derivatives as polyelectrolytes in layer-by-layer processing materials – a review, Carbohydr. Polym. 293 (2022) 119700, https://doi.org/10.1016/j.carbpol.2022.119700.

[49] Q. Shen, Y. Guo, K. Wang, C. Zhang, Y. Ma, A review of chondroitin sulfate's preparation, properties, functions, and applications, Molecules 28 (2023) 7093, https://doi.org/10.3390/molecules28207093.

[50] P. Wang, L. Chi, Z. Zhang, H. Zhao, F. Zhang, R.J. Linhardt, Heparin: an old drug for new clinical applications, Carbohydr. Polym. 295 (2022) 119818, https://doi.org/10.1016/j.carbpol.2022.119818.

[51] T.U. Jayawardena, D.P. Nagahawatta, I.P.S. Fernando, Y.T. Kim, J.S. Kim, W.S. Kim, J.S. Lee, Y.J. Jeon, A review on fucoidan structure, extraction techniques, and its role as an immunomodulatory agent, Mar. Drugs 20 (2022) 755, https://doi.org/10.3390/md20120755.

[52] S.T. Minzanova, V.F. Mironov, D.M. Arkhipova, A.V. Khabibullina, L.G. Mironova, Y.M. Zakirova, V.A. Milyukov, Biological activity and pharmacological application of pectic polysaccharides: a review, Polymers 10 (2018) 1407, https://doi.org/10.3390/polym10121407.

[53] M.H. Azarian, W. Sutapun, Tuning polymorphs of precipitated calcium carbonate from discarded eggshells: effects of polyelectrolyte and salt concentration, RSC Adv. 12 (2022) 14729–14739, https://doi.org/10.1039/d2ra01673g.
[54] M.H. Azarian, T. Junyusen, W. Sutapun, Biogenic vaterite calcium carbonate-silver/poly(vinyl alcohol) film for wound dressing, ACS Omega 9 (2023) 955–969, https://doi.org/10.1021/acsomega.3c07135.
[55] S.V. Singh, P.N. Viswanathan, Q. Rahman, Interaction between erythrocyte plasma membrane and silicate dusts, Environ. Health Perspect. 51 (1983) 55–60, 0.1289/ehp.835155.
[56] D.S.G. Nielsen, M. Fredborg, V. Andersen, A.K. Nielsen, P.K. Theil, S. Purup, Reversible effect of dextran sodium sulfate on mucus secreting intestinal epithelial cells, J. Anim. Sci. 94 (2016) 467–471, https://doi.org/10.2527/jas.2015-9737.
[57] L. Ma, X. Zhang, C. Zhang, B. Hou, H. Zhao, FOSL1 knockdown ameliorates DSS-induced inflammation and barrier damage in ulcerative colitis via MMP13 downregulation, Exp. Ther. Med. 24 (2022) 551, https://doi.org/10.3892/etm.2022.11488.
[58] C.G. Kontoyannis, V.V. Nikos, Calcium carbonate phase analysis using XRD and FT-Raman, Analyst 125 (2000) 251–255, https://doi.org/10.1039/a908609i.
[59] N.G. Balabushevich, E.A. Kovalenko, L.N. Maltseva, L.Y. Filatova, D.V. Moysenovich, E.V. Mikhalchik, D. Volodkin, A.S. Vikulina, Immobilisation of antioxidant enzyme catalase on porous hybrid microparticles of vaterite with mucin, Adv. Eng. Mat. 24 (2022) 2101797, https://doi.org/10.1002/adem.202101797.
[60] N.G. Balabushevich, E.A. Kovalenko, L.Y. Filatova, E.A. Kirzhanova, E.V. Mikhalchik, D. Volodkin D, A.S. Vikulina, Hybrid mucin–vaterite microspheres for delivery of proteolytic enzyme chymotrypsin, Macromol. Biosci. 22 (2022) e2200005, https://doi.org/10.1002/mabi.202200005.
[61] S. Popov, N. Paderin, E. Chistiakova, D. Ptashkin, P.A. Markov, Effect of cross-linking cations on in vitro biocompatibility of apple pectin gel beads, Int. J. Mol. Sci. 23 (2022) 14789, https://doi.org/10.3390/ijms232314789.
[62] L. Cao, W. Lu, A. Mata, K. Nishinari, Y. Fang, Egg-box model-based gelation of alginate and pectin: a review, Carbohydr. Polym. 242 (2020) 116389, https://doi.org/10.1016/j.carbpol.2020.116389.
[63] D.B. Trushina, T.V. Bukreeva, M.N. Antipina, Size-controlled synthesis of vaterite calcium carbonate by the mixing method: aiming for nanosized particles, Cryst. Growth Des. 16 (3) (2016) 1311–1319, https://doi.org/10.1021/acs.cgd.5b01422.
[64] S.L. Costa, G.P. Fidelis, S.L. Cordeiro, R.M. Oliveira, D.A. Sabry, R.B. Câmara, L.T. Nobre, M.S. Costa, J. Almeida-Lima, E.H. Farias, E.L. Leite, H.A. Rocha, Biological activities of sulfated polysaccharides from tropical seaweeds, Biomed. Pharmacother. 64 (2010) 21–28, https://doi.org/10.1016/j.biopha.2009.03.005.
[65] K.R. Melo, R.B. Camara, M.F. Queiroz, A.A. Vidal, C.R. Lima, R.F. Melo-Silveira, J. Almeida-Lima, H.A. Rocha, Evaluation of sulfated polysaccharides from the brown seaweed Dictyopteris justii as antioxidant agents and as inhibitors of the formation of calcium oxalate crystals, Molecules 18 (2013) 14543–14563, https://doi.org/10.3390/molecules181214543.
[66] K.D.C.M. de Melo, L.D.S. Lisboa, M.F. Queiroz, W.S. Paiva, A.C. Luchiari, R.B.G. Camara, L.S. Costa, H.A.O. Rocha, Antioxidant activity of fucoidan modified with gallic acid using the redox method, Mar. Drugs 20 (2022) 490, https://doi.org/10.3390/md20080490.
[67] M.M.C.L. Silva, L. Dos Santos Lisboa, W.S. Paiva, L.A.N.C. Batista, A.C. Luchiari, H.A.O. Rocha, R.B.G. Camara, Comparison of in vitro and in vivo antioxidant activities of commercial fucoidans from Macrocystis pyrifera, Undaria pinnatifida, and Fucus vesiculosus, Int. J. Biol. Macromol. 216 (2022) 757–767, https://doi.org/10.1016/j.ijbiomac.2022.07.110.
[68] A. Benslima, S. Sellimi, M. Hamdi, R. Nasri, M. Jridi, D. Cot, S. Li, M. Nasri, N. Zouari, Brown seaweed *Cystoseiraschiffneri* as a promising source of sulfated fucans: seasonal variability of structural, chemical, and antioxidant properties, Food Sci. Nutr. 16 (2021) 1551–1563, https://doi.org/10.1002/fsn3.2130.
[69] D. Lapenna, A. Mezzetti, S. de Gioia, G. Ciofani, L. Marzio, C. Di Ilio, F. Cuccurullo, Heparin: does it act as an antioxidant in vivo? Biochem. Pharmacol. 44 (1992) 188–191, https://doi.org/10.1016/0006-2952(92)90057-.
[70] E. Illés, A. Mizrahi, V. Marks, D. Meyerstein, Carbonate-radical-anions, and not hydroxyl radicals, are the products of the Fenton reaction in neutral solutions containing bicarbonate, Free Radic. Biol. Med. 131 (2019) 1–6, https://doi.org/10.1016/j.freeradbiomed.2018.11.015.
[71] M. Carlsson, J. Lind, G. Merényi, A selectivity study of reaction of the carbonate radical anion with methyl β-d-cellobioside and methyl β-d-glucoside in oxygenated aqueous solutions, Holzforschung 60 (2006) 130, https://doi.org/10.1515/HF.2006.021.
[72] O.V. Khorolskyi, N.P. Malomuzh, Macromolecular sizes of serum albumins in its aqueous solutions, AIMS Biophysics 7 (2020) 219–235, https://doi.org/10.3934/biophy.2020017.
[73] E.M. Collnot, H. Ali, C.M. Lehr, Nano- and microparticulate drug carriers for targeting of the inflamed intestinal mucosa, J. Control. Release 161 (2012) 235–246, https://doi.org/10.1016/j.jconrel.2012.01.028.
[74] Nidhi, M. Rashid, V. Kaur, S.S. Hallan, S. Sharma, N. Mishra, Microparticles as controlled drug delivery carrier for the treatment of ulcerative colitis: a brief review, Saudi Pharm. J. 24 (2016) 458–472, https://doi.org/10.1016/j.jsps.2014.10.001.
[75] K. Ishisono, T. Mano, T. Yabe, K. Kitaguchi, Dietary fiber pectin ameliorates experimental colitis in a neutral sugar side chain-dependent manner, Front. Immunol. 10 (2019) 2979, https://doi.org/10.3389/fimmu.2019.02979.
[76] A. Iraha, H. Chinen, A. Hokama, T. Yonashiro, T. Kinjo, K. Kishimoto, M. Nakamoto, T. Hirata, N. Kinjo, F. Higa, M. Tateyama, F. Kinjo, J. Fujita, Fucoidan enhances intestinal barrier function by upregulating the expression of claudin-1, World J. Gastroenterol. 19 (2013) 5500–5507, https://doi.org/10.3748/wjg.v19.i33.5500.
[77] S. Jarmakiewicz-Czaja, K. Ferenc, A. Sokal-Dembowska, R. Filip, Nutritional support: the use of antioxidants in inflammatory bowel disease, Int. J. Mol. Sci. 25 (2024) 4390, https://doi.org/10.3390/ijms25084390.
[78] S. Zeerleder, T. Mauron, B. Lämmle, W.A. Wuillemin, Effect of low-molecular weight dextran sulfate on coagulation and platelet function tests, Thromb. Res. 105 (2002) 441–446, https://doi.org/10.1016/s0049-3848(02)00041-5.
[79] C.B. Srikanth, P.V. Salimath, C.D. Nandini, Erythrocytes express chondroitin sulphate/dermatan sulphate, which undergoes quantitative changes during diabetes and mediate erythrocyte adhesion to extracellular matrix components, Biochimie 94 (2012) 1347–1355, https://doi.org/10.1016/j.biochi.2012.03.002.
[80] K. Ozaltin, M. Lehocký, P. Humpolíček, J. Pelková, P. Sáha, A new route of fucoidan immobilization on low density polyethylene and its blood compatibility and anticoagulation activity, Int. J. Mol. Sci. 17 (2016) 908, https://doi.org/10.3390/ijms17060908.
[81] E. Mikhalchik, L.Y. Basyreva, S.A. Gusev, O.M. Panasenko, D.V. Klinov, N.A. Barinov, O.V. Morozova, A.P. Moscalets, L.N. Maltseva, L.Y. Filatova, E.A. Pronkin, J.A. Bespyatykh, N.G. Balabushevich, Activation of neutrophils by mucin-vaterite microparticles, Int. J. Mol. Sci. 23 (2022) 10579, https://doi.org/10.3390/ijms231810579.
[82] E.V. Mikhalchik, L.N. Maltseva, R.K. Firova, M.A. Murina, I.V. Gorudko, D.V. Grigorieva, V.A. Ivanov, E.A. Obraztsova, D.V. Klinov, E.V. Shmeleva, S.A. Gusev, O.M. Panasenko, A.V. Sokolov, N.P. Gorbunov, L.Y. Filatova, N.G. Balabushevich, Incorporation of pectin into vaterite microparticles prevented effects of adsorbed mucin on neutrophil activation, Int. J. Mol. Sci. 24 (2023) 15927, https://doi.org/10.3390/ijms242115927.
[83] B. Chatterjee, N. Amalina, P. Sengupta, U.K. Mandal, Mucoadhesive polymers and their mode of action: a recent update, J. Appl. Pharm. Sci. 7 (2017) 195–203, https://doi.org/10.7324/JAPS.2017.70533.
[84] Y. Zhang, P. Ma, Y. Wang, J. Du, Q. Zhou, Z. Zhu, X. Yang, J. Yuan, Biocompatibility of porous spherical calcium carbonate microparticles on Hela cells, World J. Nano Sci. Eng. 2 (2012) 25–31, https://doi.org/10.4236/wjnse.2012.21005.
[85] E.M. Danielsen, A. De Haro Hernando, M. Yassin, K. Rasmussen, J. Olsen, G.H. Hansen, E.M. Danielsen, Short-term tissue permeability actions of dextran sulfate sodium studied in a colon organ culture system, Tissue Barriers 2 (2020) 728165, https://doi.org/10.1080/21688370.2020.1728165.